AIP | Journal of Applied Physics

Electronic and thermoelectric analysis of phases in the In2O3(ZnO)k system

E. Mitchell Hopper, Qimin Zhu, Jung-Hwan Song, Haowei Peng, Arthur J. Freeman et al.

Citation: J. Appl. Phys. 109, 013713 (2011); doi: 10.1063/1.3530733
View online: http://dx.doi.org/10.1063/1.3530733
View Table of Contents: http://jap.aip.org/resource/1/JAPIAU/v109/i1
Published by the American Institute of Physics.

Electronic and thermoelectric analysis of phases in the $In_2O_3(ZnO)_k$ system

E. Mitchell Hopper,[1,a)] Qimin Zhu,[1] Jung-Hwan Song,[2] Haowei Peng,[2] Arthur J. Freeman,[2] and Thomas O. Mason[1]
[1]*Department of Materials Science and Engineering, Northwestern University, Evanston, Illinois 60208, USA*
[2]*Department of Physics and Astronomy, Northwestern University, Evanston, Illinois 60208, USA*

(Received 14 October 2010; accepted 17 November 2010; published online 13 January 2011)

The high-temperature electrical conductivity and thermopower of several compounds in the $In_2O_3(ZnO)_k$ system (k=3, 5, 7, and 9) were measured, and the band structures of the k=1, 2, and 3 structures were predicted based on first-principles calculations. These phases exhibit highly dispersed conduction bands consistent with transparent conducting oxide behavior. Jonker plots (Seebeck coefficient versus natural logarithm of conductivity) were used to obtain the product of the density of states and mobility for these phases, which were related to the maximum achievable power factor (thermopower squared times conductivity) for each phase by Ioffe analysis (maximum power factor versus Jonker plot intercept). With the exception of the k=9 phase, all other phases were found to have maximum predicted power factors comparable to other thermoelectric oxides if suitably doped. © *2011 American Institute of Physics*. [doi:10.1063/1.3530733]

I. INTRODUCTION

The increased attention in recent years on thermoelectric power generation via waste heat reclamation has driven a search for new or improved thermoelectric materials. It is particularly important to develop thermoelectric materials that are effective at the high temperatures (500–1000 °C) necessary for power generation applications.[1]

The most useful criterion to determine the thermoelectric performance of a material is the dimensionless figure of merit (ZT):[2]

$$ZT = \frac{\alpha^2\sigma}{\kappa}T. \quad (1)$$

In this equation, α is the thermopower (or Seebeck coefficient), σ is the electrical conductivity, κ is the thermal conductivity, and T is the temperature. The term $\alpha^2\sigma$ is called the power factor (PF).

Based on Eq. (1), it is apparent that thermoelectric performance generally increases with temperature. Alloys and compounds with high carrier mobilities, e.g., Si–Ge alloys,[3] metal chalcogenides,[4,5] transition metal disilicides,[6,7] and B-based compounds[8,9] have been developed as high temperature thermoelectrics but chemical instability at elevated temperatures (i.e., oxidation, decomposition, or vaporization of a key component) tends to limit their use.[10] Additionally, while ZT generally increases with temperature, the figure of merit for most conventional thermoelectrics reaches a peak at a certain temperature and then quickly declines. This is caused by promotion of intrinsic minority carriers across the band gap at high temperature and a corresponding shift in the Fermi level toward mid-gap, which results in a decreased thermopower.[11]

Recent results show that transparent conducting oxides (TCOs) are a promising alternative to these traditional high-temperature thermoelectric materials. Oxides possess excellent structural and chemical stability at elevated temperatures. TCOs in particular possess high density of states (DOS)-mobility products (see below), which lead to high power factors. Another significant advantage of TCOs is that they possess wide band gaps ($E_g \geq 3.1$ eV),[12] which prevent thermal excitation of carriers and thus allow ZT to continue to increase at high temperatures. For example, bulk La-doped $SrTiO_3$ has a ZT value of 0.27 at 1073 K (Ref. 13) and ZnO codoped with Al and Ga has a reported ZT value of 0.65 at 1247 K.[14] Even higher ZT values have been reported for epitaxial thin films and superlattices (up to $ZT \approx 2.4$ at 300 K for $SrTiO_3$-based materials).[15]

One promising thermoelectric oxide system is the series of homologous or layered In–Zn–O (IZO) compounds with the formula $In_2O_3(ZnO)_k$, where k is an integer. These phases consist of alternating layers of In–O octahedra and In, Zn, and O in a wurtzite-like structure; in effect, they form a natural superlattice.[16] The layered nature is thought to impart a low thermal conductivity to the structure, as has been observed in the high-ZT p-type Na-based and Ca-based cobalt oxide systems.[1,17] For example, thermal conductivities as low as 2–2.5 W/mK have been reported for doped homologous $In_2O_3(ZnO)_k$ (k=3, 4, and 5) at 1000 °C,[18,19] while similarly doped specimens of the component oxides In_2O_3 and ZnO have greater thermal conductivity at the same temperature.[20,21]

Owing to the wide variety of potential thermoelectric oxide candidates to be investigated and the incomplete literature regarding thermoelectric properties of the $In_2O_3(ZnO)_k$ homologous phases, especially at high temperature, it is desirable to rapidly establish how much the thermoelectric properties of this particular system can be increased through optimization (e.g., choice of phase and doping level). One such screening method utilizes a technique developed by Jonker[22] to obtain the DOS-mobility product, an important electrical property for semiconductors. This quantity can be related to the maximum achievable power factor for a given material system through an approach originally presented by

a)Electronic mail: e-hopper@northwestern.edu.

Ioffe.[23] Combined Jonker and Ioffe analysis was recently applied to several transparent conducting and semiconducting oxide systems.[24] The current work uses this analysis to assess the thermoelectric performance of the k=1, 2, 3, 5, 7, and 9 phases in the $In_2O_3(ZnO)_k$ system. Because the k=1 phase, to the authors' knowledge, has not been successfully synthesized by conventional solid state methods and the k=2 phase is unstable in bulk form below 1550 °C,[25] these phases were analyzed based on first-principles calculations of their electrical properties. First-principles calculations were also performed on the k=3 phase for comparison with experimental data.

II. EXPERIMENTAL PROCEDURE

Bulk polycrystalline samples of $In_2O_3(ZnO)_k$ (k=3, 5, 7, and 9) were obtained by conventional solid state synthesis. The starting powders (In_2O_3, 99.99%, and ZnO, 99.999%, Alfa Aesar, Ward Hill, MA) were thoroughly mixed and pressed into pellets, which were calcined at 1000 °C for 12 h in air. To limit Zn loss due to vaporization and contamination from the crucible wall at high temperatures, each pellet was surrounded by a bed of sacrificial powder of the same composition and placed inside several nested crucibles. After the calcination step the pellets were ground and repressed, then sintered at 1300 °C for 24 h. The k=5, 7, and 9 pellets were cooled slowly (6 °C/min), and the k=3 pellets were air quenched because the phase is unstable below 1250 °C.[26] The density of each pellet was determined by dividing the mass by the calculated volume. Phase purity of the sintered pellets was confirmed by x-ray diffraction with a Rigaku diffractometer (Rigaku, Inc., Tokyo, Japan) using a Cu K_α source.

Optical band gaps were measured via diffuse reflectance, a technique analogous to transmission measurements for thin films, using a Lambda 1050 UV/Vis/NIR spectrophotometer with an integrating sphere attachment (PerkinElmer, Oak Brook, IL). Spectra were taken from 200 to 800 nm and a baseline spectrum was taken using pressed polytetrafluoroethylene powder compacts. The band gaps were estimated from the absorption edges of the diffuse reflectance spectra.

Electrical conductivity and thermopower measurements, as described by Hong, *et al.*,[27] were used to characterize the thermoelectric properties of each sample at 750 °C. Four-point conductivity measurements using S-type thermocouples for electrodes were performed on bar-shaped samples cut from the sintered ceramic pellets. The thermocouples allowed for simultaneous measurement of the thermopower. Conductivity measurements were corrected for porosity using the Bruggeman symmetric model[28] and averaged between forward and reverse current to account for the Seebeck voltage generated along the length of the sample.

Typically the carrier content variation required for Jonker analysis is achieved by preparing samples with a range of doping levels. However, due to the relatively small effect of aliovalent doping on carrier concentration in the IZO homologous phases,[29] for this experiment the carrier content was varied by letting each sample equilibrate under different oxygen partial pressures (pO_2). The pO_2 was varied between 21% and 0.01% (100 ppm) O_2, obtained by using mixtures of argon and oxygen, and confirmed by a Thermox CG 1000 oxygen analyzer (Ametek Inc., Paoli, PA). Conductivity and thermopower measurements were taken after both had reached their equilibrium value for each pO_2, which typically took several days to achieve.

III. THEORETICAL PROCEDURE

The band structures and electrical properties of the k=1, 2, and 3 phases (Fig. 1) were calculated by established first-principles methodologies. These structures were investigated using the highly precise full-potential linearized augmented plane wave (FLAPW) method,[30–32] with no artificial shape approximation for the wave functions, charge densities, or potentials. The atomic structures employed in this work, as shown in Fig. 2, were provided by Da Silva *et al.*[16] and were obtained by first-principles calculations. Regular local density approximation (LDA) calculations were first performed using the exchange-correlation potential with the Hedin–Lundvist parameterization.[33] Core states were treated fully relativistically and updated at each iteration, while the valence states were treated semirelativistically. The radius of muffin-tin (MT) spheres were set to 2.1 Bohr, 2.0 Bohr, and 1.62 Bohr for In, Zn, and O, respectively. Cutoffs of the plane-wave basis (4.5 Ry) and potential representation (12.0 Ry), and the expansion in terms of spherical harmonics with $l \leq 8$ inside the MT spheres were used for the LDA-FLAPW calculations. Initially, summations over the Brillouin zone were done using a $6\times5\times4$ Monkhorst–Pack[34] k-mesh for the k=1 structure, a $6\times5\times2$ k-mesh for k=2, and a $3\times5\times2$ k-mesh for k=3. Then, self-consistent screened-exchange LDA (sX-LDA) (Ref. 35) calculations were carried out based on the converged LDA results, to overcome the LDA band gap error. The s and p electrons were included in the screening, and cut-off parameters of 3.1 Ry in the wave vectors and $l \leq 4$ inside the MT spheres were chosen. Due to the heavy computational demands, the k-mesh used in the sX-LDA calculations was reduced to $4\times4\times2$ for the k=1 structure, $4\times4\times1$ for k=2, and $2\times4\times1$ for k=3.

A. Jonker and Ioffe analysis

To maximize the figure of merit for a given material, it is desirable to have the highest power factor ($\alpha^2\sigma$) possible. However, electrical conductivity decreases as thermopower increases. Given this tradeoff, it is necessary to determine the optimum combination of the two properties that will maximize the material's power factor, and the value of the maximum achievable power factor.

For a nondegenerate n-type semiconductor, the thermopower (α) can be described by:[22]

$$\alpha = -\frac{k}{e}\left(\ln\frac{N_c}{n} + A\right). \tag{2}$$

In this equation, k is Boltzmann's constant, e is the electronic charge, N_c is the DOS, n is the carrier concentration, and A is a transport constant that depends upon the dominant scattering mechanism.

This can be combined with the expression for conductivity in terms of mobility (μ) and carrier concentration (n):

$$\sigma = ne\mu, \tag{3}$$

to yield:

$$\alpha = \frac{k}{e}(\ln\sigma - \ln\sigma_0), \tag{4}$$

where σ_0 is given by:

$$\sigma_0 = N_c e \mu e^A. \tag{5}$$

Thus, a plot of α versus $\ln\sigma$, called a "Jonker plot," will have a slope of k/e (86.15 μV/K), with its intercept on the $\ln\sigma$ axis at $\ln\sigma_0$. This intercept will be referred to as the "DOS-mobility product," since these two parameters largely govern its value.

By substituting Eqs. (3) and (4) into the power factor ($\alpha^2\sigma$) and differentiating with respect to $\ln\sigma_0$, it is possible to predict the maximum power factor (PF_{max}) that can be achieved within a given material system. This maximum occurs when $\ln\sigma = \ln\sigma_0 - 2$ and is described by the following equation:[23]

$$\ln PF_{max} = ln\left[4\left(\frac{k}{e}\right)^2\right] - 2 + \ln\sigma_0 \approx -19.33 + \ln\sigma_0, \tag{6}$$

where PF is the power factor. Note that σ must be in siemens per meter for this equation to be valid.

This relationship is significant when considering practical requirements for thermoelectric materials. Jonker plots enable the value of the DOS-mobility product ($\ln\sigma_0$) to be established. Equation (6) then allows the PF_{max} to be estimated. This sets the minimum value of thermal conductivity required to achieve acceptable thermoelectric performance, typically $ZT \geq 1$. For example, the lowest reported thermal conductivities for oxides like those in the present study are on the order of 1 W/mK.[36,37] To achieve ZT=1 at 1000 K, a material with this thermal conductivity would require $\ln\sigma_0 = 12.4$ or $PF_{max} = 10^{-3}$ W/mK^2. If the $\ln\sigma_0$ calculated from the Jonker plot is below 12.4, the figure of merit for this material system cannot exceed 1 at this temperature. In this way, it is possible to determine how large a figure of merit is possible for a given material system at a temperature of interest.

IV. RESULTS AND DISCUSSION

A. Theoretical calculations

The band structures of $In_2O_3(ZnO)_k$ (k=1, 2, 3), from both the LDA and sX-LDA calculations, are shown in Fig. 1. The LDA/sX-LDA band gaps are presented in Table I along with experimental band gaps measured by diffuse reflectance. It can be seen that the sX-LDA band gap values (2.6–3.1 eV) are a distinct improvement over the LDA-based values (0.6–0.9 eV) and in much better agreement with experimental values. In particular, the sX-LDA band gap of the k=3 phase (~3.0 eV) is in reasonable agreement with the diffuse reflectance result (~2.7 eV). The k=1 phase has an indirect band gap from Z to Γ, which is 0.129/0.108 eV smaller than the direct band gap at the Γ point in the LDA/sX-LDA calculations. As shown in the band structure plots, the conduction bands of all the three oxides are much more dispersive than the valence bands, which is related to their potential application as n-type TCOs. For the odd k phases, the top valence bands are very flat in all three directions. For the k=2 phase, there is a notable anisotropic phenomenon. From Γ to X (or Y) there is obvious band dispersion which is not exhibited by the odd phases, while from Γ to Z the top valence bands are so flat that they are totally separated from the rest of the valence bands. This phenomenon can be attributed to the In-free layers with fivefold coordinated Zn atoms which only exist in the k=2 phase, as denoted with a dashed rectangle in Fig. 2(b). Indeed, after plotting the site-projected DOS, it can be seen that these states are mostly dominated by Zn *d* and O *p* states from the pure Zn–O layers.

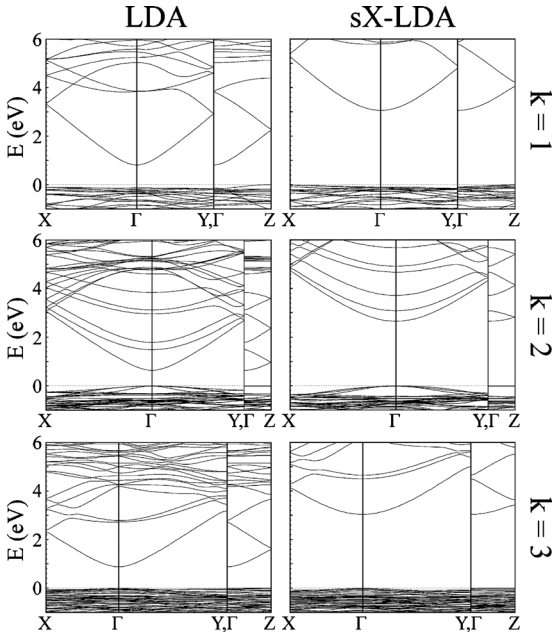

FIG. 1. The LDA and sX-LDA band structures for $In_2O_3(ZnO)_k$ (k=1, 2, 3), where Γ is the center of the Brillouin zone, X=(0.5,0.0,0.0), Y=(0.0,0.5,0.0), and Z=(0.0,0.0,0.5). The energy zero is set at the valence band maximum.

To theoretically investigate the transport properties such as Seebeck coefficient (α) and electrical conductivity (σ), and to understand their relationship with the electronic structure, the Boltzmann transport expression in the constant re-

TABLE I. Band gaps of $In_2O_3(ZnO)_k$ phases obtained by LDA and sX-LDA calculations or measured by diffuse reflectance.

	Band gap (eV)		
$In_2O_3(ZnO)_k$ compound	LDA	sX-LDA	Diffuse Reflectance
k=1	0.811	3.060	···
k=2	0.636	2.642	···
k=3	0.877	3.036	2.72
k=5	···	···	2.75
k=7	···	···	2.82
k=9	···	···	2.83

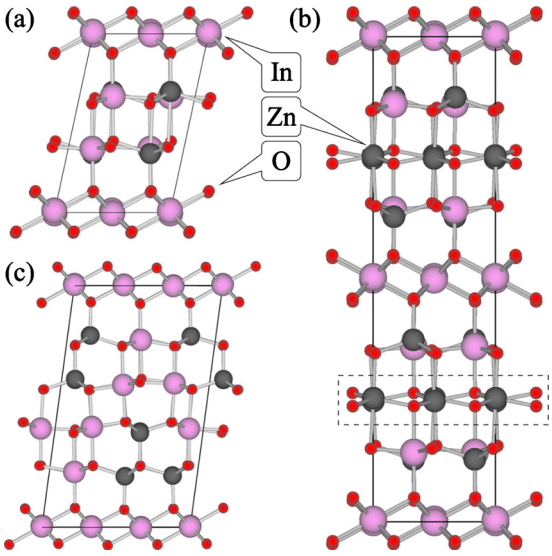

FIG. 2. (Color online) The atomic structures of $In_2O_3(ZnO)_k$ viewed along the [010] direction: (a) k=1, (b) k=2, and (c) k=3. The In, Zn, and O atoms are represented with pink (large), gray (medium), and red (small) balls (Ref. 43).

laxation time approximation was employed.[38] The constant relaxation time was found by fitting the calculated results to an experimental data point for the k=3 phase (α=−438 μV/K, $\sigma=1.15\times10^3$ S/m) and was found to be 10^{-14} s, a typical value for oxides. Full intraband optical matrix elements[38] calculated with the FLAPW method were used to determine the group velocities used in the transport coefficients. Different carrier concentrations for the transport coefficient calculations were treated within the rigid band model, and the Fermi–Dirac distribution function at 1025 K was used for the temperature contribution. It was found that the calculated thermopowers and conductivities were nearly identical for the k=1, 2, and 3 phases. These observations help to explain the roughly k-independent thermoelectric properties of the system, discussed below.

B. Combined experimental/theoretical results

The experimental conductivity and thermopower for the k=3 sample are plotted together with the calculated values as a Jonker plot in Fig. 3. The scatter in the experimental values may be attributed to increased grain boundary scattering at small carrier content. A better experimental result was achieved for the k=5 phase, shown in Fig. 4. The Jonker plot-derived values of the DOS-mobility product for each compound are presented in Table II. Values for the k=3 phase are based on the combination of experimental and calculated results.

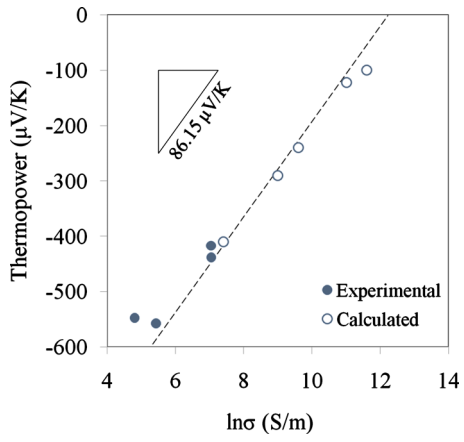

FIG. 3. (Color online) Jonker plot of the $In_2O_3(ZnO)_3$ phase at 750 °C, showing experimentally measured values (closed circles) and values predicted by band structure calculations (open circles). Carrier concentrations used for the calculations were between 10^{18} cm^{-3} and 10^{20} cm^{-3}.

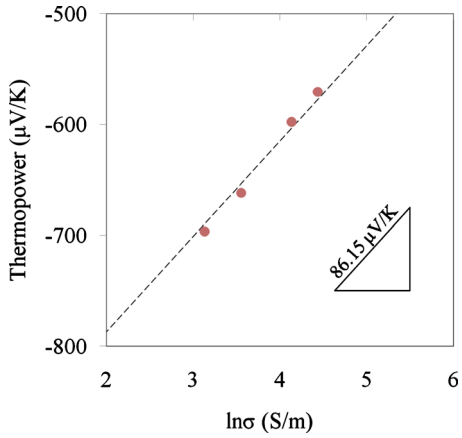

FIG. 4. (Color online) Jonker plot of the $In_2O_3(ZnO)_5$ phase at 750 °C.

A generous ±50% uncertainty in the DOS-mobility products has been incorporated in Table II, considering the porous, polycrystalline nature of our specimens. Although we did not see evidence of major changes in grain size or texturing from sample to sample, these factors can also contribute to uncertainty in conductivity. Nevertheless, we obtained good agreement between the predicted PF_{max} and the best reported power factors in the literature (see Table II).

Based on the range of DOS-mobility products ($\ln\sigma_0$) determined from Jonker plots, the range of corresponding PF_{max} for each k-phase was included in the Ioffe plot (Fig. 5). From this figure, it is clear that the maximum predicted power factors are very similar for all phases, with the possible exception of k=9.

The k=5 phase has been the most extensively studied with regard to the effect of dopant type, doping level, and texturing on its thermoelectric properties.[19,39–42] The highest reported power factor for this phase [5.2×10^{-4} W/mK^2

TABLE II. DOS-mobility product ranges and the corresponding PF_{max} predicted by Ioffe analysis, as well as the highest reported PF from the literature, for several $In_2O_3(ZnO)_k$ phases, In_2O_3:Sn (ITO), ZnO:Al, and $SrTiO_3$:Nb at 1053–1073 K.

Material	$\ln\sigma_0$ (S/m)	Predicted PF_{max} (10^{-4} W/mK^2)	Best reported PF (10^{-4} W/mK^2)
IZO k=1	11.8–12.9	5.5–15.0	···
IZO k=2	11.8–12.9	5.5–15.0	···
IZO k=3	11.5–12.6	4.0–12.0	4.8 (Ref. 39)
IZO k=5	10.4–11.5	1.4–4.1	5.2 (Ref. 19)
IZO k=7	11.2–12.3	3.0–8.9	3.2 (Ref. 39)
IZO k=9	10.0–11.1	0.9–2.7	2.7 (Ref. 39)
In_2O_3:Sn	11.1–12.2 (Ref. 24)	2.7–8.0 (Ref. 24)	7.1 (Ref. 24)
ZnO:Al	11.7–12.8 (Ref. 10)	4.7–14.2 (Ref. 24)	14.4 (Ref. 10)
$SrTiO_3$:Nb	11.9–13.0 (Ref. 13)	6.1–18.4 (Ref. 24)	5.7 (Ref. 13)

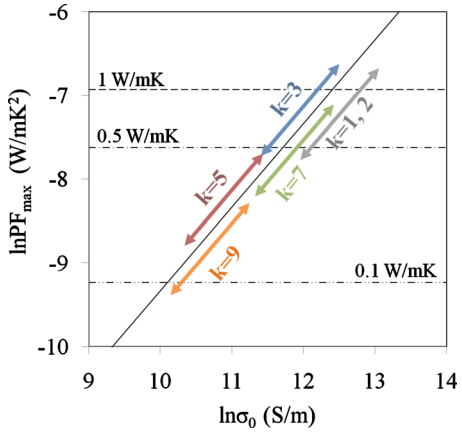

FIG. 5. (Color online) Ioffe plot (ln PF_{max} vs lnσ_0) for the $In_2O_3(ZnO)_k$ phases (k=1, 2, 3, 5, 7, 9). The dashed lines indicate the thermal conductivity necessary to achieve a ZT equal to 1 at 1000 K as a function of power factor.

(Ref. 19)] is somewhat higher than the maximum range predicted in the present study. We suspect this is attributable to optimization of texturing in Ref. 19, whereas the specimens in the present work are largely untextured. What is significant about the present work is that the other k-phases have been largely overlooked for high temperature thermoelectric applications, but all are predicted to be able to achieve similar thermoelectric performance. Note that the best reported power factors for k=3, 5, 7, and 9 are all on the same order as that for Nb-doped $SrTiO_3$, though still significantly less than that of Al-doped ZnO.

It should be emphasized that the best k-phase thermoelectrics, based upon power factors only, involve extrinsic donor-doping. In the present work, the maximum achievable power factors for these compounds were estimated based upon pO_2 variations in electrical properties ($k \geq 3$) and theoretical calculations vs. carrier content ($k \leq 3$) in nominally undoped compounds. This demonstrates the potential of combined Jonker/Ioffe analyses for "predicting" optimum thermoelectric properties once appropriate donors have been identified.

V. CONCLUSIONS

Electronic and thermoelectric properties of compounds in the $In_2O_3(ZnO)_k$ system have been analyzed by a combined theoretical and experimental approach. The k=1 and 2 phases, which have not been studied in bulk form, were investigated by LDA and sX-LDA band structure calculations. Calculations were also performed on the k=3 phase to compare with experimental results. Band structure calculations confirmed a highly dispersed conduction band for these phases, which accounts for their TCO behavior. The band gap calculated by sX-LDA showed reasonable agreement with that measured by diffuse reflectance for the k=3 phase. The DOS-mobility products predicted by Jonker analysis of the calculated thermopowers and conductivities were nearly identical for all three phases and were similar to those calculated for the other phases based on experimental measurements.

The thermopower and conductivity of the k=3, 5, 7, and 9 phases were measured at 750 °C while varying the carrier concentration by equilibrating the samples under different oxygen partial pressures. Jonker analysis was used to calculate the DOS-mobility product for each phase based on the measured thermopower and conductivity, and Ioffe analysis related the DOS-mobility product to the maximum achievable power factor for each compound. The ranges of maximum power factor predicted for each phase were in good agreement with the highest reported power factors in the literature, demonstrating the usefulness of combined Jonker and Ioffe analyses for predicting the behavior of a given material system under ideal doping conditions.

With the exception of the k=9 phase, the maximum achievable power factors predicted for all phases were similar to one another. These maximum power factors are comparable to those of ITO (In_2O_3:Sn) and other TCOs being considered for thermoelectric applications. This suggests that the compounds in this system warrant further study; optimization of their electrical properties could make them viable for high temperature thermoelectric applications.

ACKNOWLEDGMENTS

This work was supported in part by the U.S. Department of Energy under Grant No. DE-FG02-08ER46536 (EMH, TOM) and Grant No. DE-SC0001050 (Energy Frontier Research Center, QZ, TOM, AJF). JHS, HP, and AJF also acknowledge support of the NSF MRSEC program under Grant No. DMR-0520513.

[1]K. Koumoto, I. Terasaki, and R. Funahashi, MRS Bull. **31**, 206 (2006).
[2]T. M. Tritt and M. A. Subramanian, MRS Bull. **31**, 188 (2006).
[3]C. Bhandari and D. Rowe, J. Contemp. Phys. **21**, 219 (1980).
[4]J. F. Nakahara, T. Takeshita, J. J. Tschetter, B. J. Beaudry, and K. A. Gschneidner, J. Appl. Phys. **63**, 2331 (1988).
[5]I. Nishida, Phys. Rev. B **7**, 2710 (1973).
[6]I. Nishida and T. Sakata, J. Phys. Chem. Solids **39**, 499 (1978).
[7]T. Kojima, Phys. Status Solidi A **111**, 233 (1989).
[8]S. Yugo, T. Sato, and T. Kimura, Appl. Phys. Lett. **46**, 842 (1985).
[9]C. Wood and D. Emin, Phys. Rev. B **29**, 4582 (1984).
[10]T. Tsubota, M. Ohtaki, K. Eguchi, and H. Arai, J. Mater. Chem. **7**, 85 (1997).
[11]L. V. Prokofieva, D. A. Pshenay-Severin, P. P. Konstantinov, and A. A. Shabaldin, Semiconductors **43**, 973 (2009).
[12]T. Minami, MRS Bull. **25**, 38 (2000).
[13]S. Ohta, T. Nomura, H. Ohta, and K. Koumoto, J. Appl. Phys. **97**, 034106 (2005).
[14]M. Ohtaki, K. Yamamoto, and K. Araki, J. Electron. Mater. **38**, 1234 (2009).
[15]H. Ohta, Mater. Today **10**, 44 (2007).
[16]J. L. F. Da Silva, Y. Yan, and S.-H. Wei, Phys. Rev. Lett. **100**, 255501 (2008).
[17]H. Ohta, K. Sugiura, and K. Koumoto, Inorg. Chem. **47**, 8429 (2008).
[18]H. Kaga, R. Asahi, and T. Tani, Jpn. J. Appl. Phys., Part 1 **43**, 7133 (2004).
[19]S. Isobe, T. Tani, Y. Masuda, W.-S. Seo, and K. Koumoto, Jpn. J. Appl. Phys., Part 1 **41**, 731 (2002).
[20]D. Berardan, E. Guilmeau, A. Maignan, and B. Raveau, Solid State Commun. **146**, 97 (2008).
[21]M. Ohtaki, T. Tsubota, and K. Eguchi, J. Appl. Phys. **79**, 1816 (1996).
[22]G. H. Jonker, Philips Res. Rep. **23**, 131 (1968).
[23]A. F. Ioffe, *Semiconductor Thermoelements and Thermoelectric Cooling* (Infosearch, London, 1957).
[24]Q. Zhu, E. M. Hopper, B. Ingram, and T. O. Mason, "Combined Jonker and Ioffe analysis of oxide conductors and semiconductors," J. Am. Ceram. Soc. (2010).

[25]V. H. Kasper, Z. Anorg. Allg. Chem. **349**, 113 (1967).
[26]T. Moriga, D. D. Edwards, T. O. Mason, G. B. Palmer, K. R. Poeppelmeier, J. L. Schindler, and C. R. Kannewurf, J. Am. Ceram. Soc. **81**, 1310 (1998).
[27]B.-S. Hong, S. J. Ford, and T. O. Mason, Key Eng. Mater. **125–126**, 163 (1997).
[28]D. S. McLachlan, M. Blaszkiewicz, and R. E. Newnham, J. Am. Ceram. Soc. **73**, 2187 (1990).
[29]T. Minami, T. Kakumu, and S. Takata, J. Vac. Sci. Technol. A **14**, 1704 (1996).
[30]E. Wimmer, H. Krakauer, M. Weinert, and A. J. Freeman, Phys. Rev. B **24**, 864 (1981).
[31]M. Weinert, E. Wimmer, and A. J. Freeman, Phys. Rev. B **26**, 4571 (1982).
[32]H. J. F. Jansen and A. J. Freeman, Phys. Rev. B **30**, 561 (1984).
[33]L. Hedin and B. I. Lundqvist, J. Phys. C **4**, 2064 (1971).
[34]H. J. Monkhorst and J. D. Pack, Phys. Rev. B **13**, 5188 (1976).
[35]D. M. Bylander and L. Kleinman, Phys. Rev. B **41**, 7868 (1990).
[36]A. Satake, H. Tanaka, and T. Ohkawa, J. Appl. Phys. **96**, 931 (2004).
[37]T. Sugahara, M. Ohtaki, and T. Souma, J. Ceram. Soc. Jpn. **116**, 1278 (2008).
[38]M. S. Park, J.-H. Song, J. E. Medvedeva, M. Kim, and A. J. Freeman, Phys. Rev. B (2010).
[39]H. Kaga, R. Asahi, and T. Tani, Jpn. J. Appl. Phys., Part 1 **43**, 3540 (2004).
[40]Y. Masuda, W.-S. Seo, W. Pitschke, and K. Koumoto, J. Solid State Chem. **150**, 221 (2000).
[41]S. Hirano, S. Isobe, T. Tani, N. Kitamura, I. Matsubara, and K. Koumoto, Jpn. J. Appl. Phys., Part 1 **41**, 6430 (2002).
[42]K. Park, K. K. Kim, J. K. Seong, S. J. Kim, J.-G. Kim, W.-S. Cho, and S. Nahm, Mater. Lett. **61**, 4759 (2007).
[43]K. Momma and F. Izumi, J. Appl. Crystallogr. **41**, 653 (2008).